Journal of Harbin Engineering University
ISSN: 1006-7043

Vol 45 No. 5
May 2024

An Effective Modified Median Filter Based on Neuman's Cellular Automata for Low SPN Attack Detection and Restoration in Medical Images

Imran Qadir[1], V Devendran[2]
[1]Computer Application, Lovely Professional University, Phagwara, Punjab, India,
[2]Computer Science and Engineering, Lovely Professional University, Phagwara, Punjab, India.

Abstract

Medical images such as brain MRI (Magnetic Resonance Imaging) scans are prone to various noise attacks. The presence of noise perplexes the identification, which may lead to inaccurate analysis and diagnosis. Under the framework of Median Filter (MF), its variant Switching Median Filter (SMF) and Cellular Automata (CA), we proposed effective Salt & Pepper Noise (SPN) filters. They work similar to those of MF and SMF except the use of Neumann Neighborhood (NN) and CA framework. Filters 1 and 2 processes all pixels in the noisy image uniformly whereas filters 3 and 4 first performs noise check and then restores the noisy pixels. Peak Signal to Noise Ratio (PSNR) performance parameter were used to test the proposed filters and the standard traditional filters. Experimental results reveal that the performance of the proposed filters is better. The proposed filters are able to restore low SPN effectively while preserving image details. The purpose of the proposed study is to present CA-based MF's so that CA-based MF's could also be explored like that of MF discussed in general image processing domain. Further, proposed filters proved computationally efficient as they required to compute lesser number of steps than standard MF and SMF by exploiting NN.

Keywords: Cellular automata, salt & pepper noise, median filter, von Neumann.

1. Introduction

The efficient and powerful computing technology used in the analysis of medical images has revolutionized the field of medical science. However, sometimes medical images captured using different imaging devices (such as MRI, CT,, X-rays and son on) get corrupted with Salt & Pepper Noise (SPN) due to low dose of rays on patient's body, pre-processing, damaged memory slots and so on [1,2,3]. Further, sometimes doctors may seek opinion from other doctors and are required to communicate images over network. Thus, there is also a possibility that attackers may attack the image with SPN. SPN is a simple and a common attack that attackers usually use to damage the image content. It is the random distribution of white and black dots on the image and can be seen from the naked eye. Presence of noise affects the quality of the image and proves to be an obstacle in the analyses and the subsequent phases such as segmentation, recognition, extraction and son on [10,11,12]. Thus, eliminating SPN from images is one of the important pre-processing steps. So in this paper, our goal was to address this problem and based upon the analysis we have proposed two SPN filters based on Cellular Automata (CA). CA are simple mathematical models originated in computer science. These models were given by John Von Neumann and Stanislaw Ulam [13, 14]. Later, researchers from different fields have implemented these models in different areas of study. Particularly, these models have been successfully studied in image processing as the structure of CA are similar to that of images [15,16,17].

In this paper, attempts have been made to present an efficient CA-based MF (Median Filter) for SPN detection and removal in brain MRI. Several similar attempts using differ methods are present in the literature. For example, SPN detection and reduction with the help of fuzzy SMF is presented in [5]. Another highly effective SPN detection and reduction algorithm on SMF is presented in [6]. A new adaptive Weighted MF for removing SPN is presented in [7]. A supervised learning algorithm for SPN detection and removal based on standard

MF is presented in [8]. Similarly, a two-stage technique for removing SPN based on directional MF is presented in [9]. The popularity of MF has inspired researchers to propose its modifications known as the variants of MF [4-9]. The goal of this study is to analyse MF so that an effective MF based on CA could be presented. In this paper, we are presenting efficient MF and SMF algorithms based on CA, known as CAMF and CASMF. CAMF consists of two phases that depends upon the noise density. If noise density is less than 10% it uses Neumann Neighborhood (NN) with radius r=1, otherwise r=2. This filter works similar to that of MF except NN. CASMF again uses two phases like in SMF. Additionally, CASMF uses noise check. That is, it first identifies the corrupted pixels and then restores it. We used two performance metrics for analysis of the proposed filters with the MF and SMF namely PSNR, and SSIM. Experimental results reveal that the proposed filters performs better visually as well as objectively. The objective of the proposed study is to propose CA-based MF's so that CA based MF's could also been explored like MF [4]. The proposed filters does not increase the number of steps rather decreases them by using CA based NN. Thus, proposed filters are also computationally efficient than MF's used in spatial domain of image processing.

This paper is organized as follows: Section (2) describes the technical preliminaries of 2d CA model. This section will lay the foundation of using CA for SPN removal. Section (3) presents the proposed filters. Section (4) presents overview of performance metrics, dataset, experimental results and discussions. This section analyzes results of the proposed filters with MF and SMF. And, finally section (5) presents the conclusions and future work of the proposed study.

2. Two Dimensional Cellular Automata

Cellular Automata (CA) are discrete mathematical models used to simulate simple to complex tasks using simple mathematical rules known as transition function. The transition functions are implemented on an infinite grid of cells known as the CA lattice. Since, images are finite, the infinite CA lattice is converted into a finite lattice by applying different boundary conditions [13,16,17]. The two most important and widely used boundary conditions are null boundary and periodic boundary. In null boundary, the image is padded with the zero values whereas in periodic boundary, the image is wrapped from one side to another side. Cells in the lattice are arranged in one, two, or in three dimensions. Each cell holds a finite value known as the initial state of the cell. The evolutions of initial CA is carried out by applying transition functions in discrete time steps and exhibited complex behaviour by local interaction. Mathematically, a CA is defined by a quadruple (L, S, N, F) [17]. Here, L represents the lattice, S represents the states of the cells, N represents the neighborhoods and F represents the transition function.

The two most important neighborhoods used in CA are shown in figure 1. Both neighborhoods are defined based upon the radius (r) measured from the main cell, that is the central cell. If r=1, means neighborhood considers the few cells among the cells whose boundary touches the boundary of the main cell. If r=1, means neighbor considers cells of r=1 as well as few cells whose boundaries touches the cells placed at r=1. First neighborhood is known as Neumann's neighborhood, NN. In this neighborhood, neighboring cells placed at top, bottom, left and right sides of the man cell are considered. Similarly the neighborhood could be extended to the next levels, that r=2,3,4,..& so on. Mathematically, NN is described in equation 1. The second neighborhood is known as the Moore neighborhood, MN. In this neighborhood, neighboring cells included in NN as well as the cells placed at diagonals are considered. Mathematically, MN is described in equation 2.

$$\delta_{1(i,j)}^{t+1} = f_{med}\{(p,q) \in CA\} \dots (2)$$

$$where, \quad (|p-i| + |q-j|) \leq r \quad \& \quad r = 1$$

$$\delta_{2(i,j)}^{t+1} = f_{med}\{(p,q) \in CA\} \dots (2)$$

$$where, \quad (|p-i| + |q-j|) \leq r \quad \& \quad r = 2$$

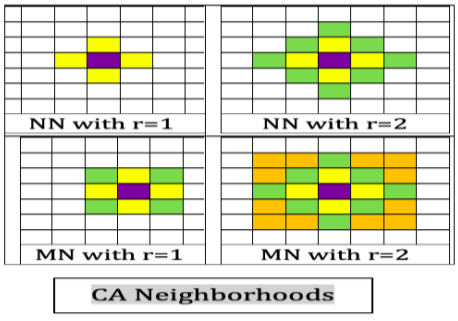

Figure 1: Two dimensional CA Neighborhoods

3. Proposed Method

Reducing noise in digital images is a process of removing unwanted data. There are different types of noise attacks ranging from Gaussian noise to SPN. So, images could be affected by different types of noises at the same time. Identification or simply removing of different noises in one image is a challenging and difficult task and there is hardly any study available for addressing multiple noises. That is the reason that researchers usually focus on one type of noise only. In this paper, we address the problem of SPN. The PDF of SPN is described in equation (1).

$$P(z) = \begin{cases} P_a & for \quad z = a \\ P_b & for \quad z = b \\ 0 & otherwise \end{cases} \quad \ldots\ldots (1)$$

MF is considered as one of the important and effective non-linear filters for removing SPN in an image while preserving image edge details. The kernel in the MF is convoluted over the entire image pixel by pixel. Pixels in the kernel are sorted in increasing order and then pixel under investigation is replaced by the median of the sorted intensities. For example, if f(x,y) represents the noisy image, the reconstructed image, g(x,y) depends on the order of the intensity values in f(x,y). The aim of this study is to investigate CA for developing effective MF.

We proposed four effective algorithms based on 2d CA for reducing SPN noise in digital images effectively, as shown in algorithms 1-4. Algorithm 1 and 2 reduces noise without first checking the pixel for noise. Thus, these algorithms treat all pixels on the CA-map equally. Although they reduce small amounts of noise effectively but at the same time they are computationally inefficient because they perform more operations unnecessarily on uncorrupted pixels. Further, applying algorithm 1 or 2 on images corrupted by higher noise densities reduces the quality of the image. Both these limitations are addressed in algorithm 3 and 4. That is, algorithms 3 and 4 first checks the pixels under investigation for impulsion and then only executes the transition function.

Mathematically, transition function for the proposed method is described in equations (2) & (3). Where f_{med} is an operator over dependent cells in the neighborhood and it computes the median value of the sorted NN. $\delta_{(i,j)}^{t+1}$ on the left-hand side of the function represents the next evolution of CA-map. The states of the cells on the CA-map is updated simultaneously by applying these two functions once or recursively.

***Algorithm* 1**: CA_MF 3*3

$step\ 1$: $I = imread('filename');$
$step\ 2$: $N = imnoise(I, 'salt\ \&\ pepper', d);$
$step\ 3$: $N = f(PBC, N);$
$step\ 4$: $for\ each\ pixel(i,j)\ \in N, do:$
$step\ 5$: $O_{i,j}^{t+1} = \delta_{1_{N(i,j)}}^{t+1};$
$step\ 6$: $end\ for$
$step\ 7$: $O = imwrite(O, 'filename')$

***Algorithm* 2**: CA_MF 5*5

$step\ 1$: $I = imread('filename');$
$step\ 2$: $N = imnoise(I, 'salt\ \&\ pepper', d);$
$step\ 3$: $N = f(PBC, N);$
$step\ 4$: $for\ each\ pixel(i,j)\ \in N, do:$
$step\ 5$: $O_{i,j}^{t+1} = \delta_{2_{N(i,j)}}^{t+1};$
$step\ 6$: $end\ for$
$step\ 7$: $O = imwrite(O, 'filename')$

***Algorithm* 3**: CA_SMF 3*3

$step\ 1$: $I = imread('filename');$
$step\ 2$: $N = imnoise(I, 'salt\ \&\ pepper', d);$
$step\ 3$: $N = f(PBC, N);$
$step\ 4$: $for\ each\ pixel(i,j)\ \in N, do:$
$step\ 5$: $if\ N_{i,j}^{t} = 0\ ||\ N_{i,j}^{t} = 1$
$step\ 6$: $O_{i,j}^{t+1} = \delta_{1_{N(i,j)}}^{t+1};$
$step\ 7$: $else$
$step\ 8$: $O_{i,j}^{t+1} = N_{i,j}^{t}$
$step\ 9$: $end\ if$
$step\ 10$: $end\ for$
$step\ 11$: $O = imwrite(O, 'filename')$

Algorithm 4: CA_SMF 5*5

step 1: $I = imread('filename');$
step 2: $N = imnoise(I,'salt \& pepper', d);$
step 3: $N = f(PBC, N);$
step 4: *for each pixel* $(i,j) \in N, do:$
step 5: *if* $N_{i,j}^{t} = 0 \,||\, N_{i,j}^{t} = 1$
step 6: $O_{i,j}^{t+1} = \delta_{2_{N(i,j)}}^{t+1};$
step 7: *else*
step 8: $O_{i,j}^{t+1} = N_{i,j}^{t}$
step 9: *end if*
step 10: *end for*
step 11: $O = imwrite(O,'filename')$

4. Experimental Results and Discussions

A brain tumor is a group or mass of abnormal growth of cells in or around the brain. The scalp around the brain is stiff. Any kind of growth inside the scalp can cause problems. The two main brain tumors are Malignant Tumor (cancerous) and Benign Tumor (non-cancerous). When these tumors grow, they cause pressure inside the scalp. This process damages the brain and it can be life threatening. Thus, early detection and classification of brain tumors is important in medical science. In this paper, our goal is to preprocess the brain MRI scans so that experts may obtain accurate results for detection and classification. In this paper, Brain Tumor MRI (BT_MRI) Dataset is used [18]. BT_MRI Dataset is a combination of three datasets namely, figshare, SARTAJ dataset and Br35H. It contains 7023 MRI scans of human brain and are classified into four types namely glioma, meningioma, no tumor and pituitary. Further, two standard test images, generally used for image processing tasks, namely lena.jpg and cameraman.jpg images have been taken for carrying out various experiments [23]. The test images which are taken for visual evaluation are shown in Figure 2. The experiments are implemented in Matlab R2016a installed on HP Desktop with Intel(R) Core (TM) i7-8700T CPU @ 2.40 GHz, 16.0 GB RAM, and Windows 64-bit Operating system.

Although performance of the algorithms used in this paper can be evaluated visually. However, mere visual assessment is not enough and not the only way [3,4,13]. There are some performance evaluation metrics that are used for efficiency assessment of algorithm objectively. In this section, one of the important quality assessment metrics namely, Peak-Signal-to-Noise-Ratio (PSNR) is presented.

PSNR is the ration between maximum intensity present in the image and density of the noise that affected the original image. It is represented in decibels and denotes the quality of the restored image. Higher PSNR value represents better image and vice versa. Mathematically, PSNR for a given noise-free image I and corrupted image N, is described in equation (2). Whereas MSE is the Mean-Square-Error that determines the average error in the restored image against the original image. Lower MSE value represents higher image quality and vice versa. MSE is described in equation (3).

$$PSNR = 10 * log_{10}\left(\frac{255^2}{MSE}\right) \ldots\ldots (2)$$

$$MSE = \frac{1}{M * N}\sum_{i=0}^{M-1}\sum_{j=0}^{N-1}[(I_{i,j} - N_{i,j})^2] \ldots (3)$$

The cropped versions of noise free and noise attacked are shown in Figure (2). It can be clearly seen in Figure 2(a) that pixels are without 0's and 1's. When image is attacked by 25% of SPN, the intensity values are transformed into extreme values and appears as the patterns of 0's and 1's, as shown in Figure 2(b). Thus, the main goal of filtering is to remove these noisy patterns/dots so that reconstructed image may approximately looks like that of the original image.

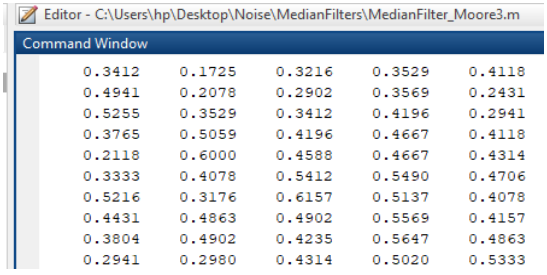

(a)

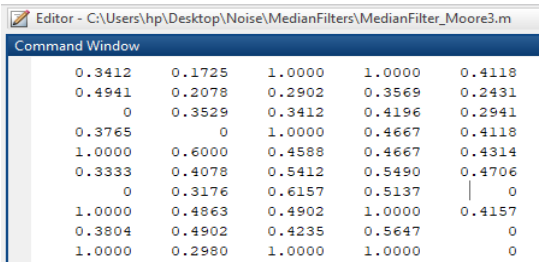

(b)

Figure 2: Cropped image; (a) noise-free image, (a) 25% noise attack.

First, we compared our proposed methods with the standard MF using two Image Processing Kernels (IPK) namely IPK (3*3) and IPK (5*5). As shown in Table 1, for MF, NN with r=1 presents better results up to 7% of noise attack as compared to the MF with IPK 3*3. Afterwards, CA_SMF with r=2 provides better results as compared to MF with IPK 5*5. Second, we compared our proposed methods with the standard SMF using the same two kernels. As shown in Table 1, again NN with r=1 presents better results up to certain noise attack whereas at noise attacks greater than 5% NN with r=2 presents better results as compared to SMF with IPK 3*3 and 5*5, respectively. As seen in the Table 1, when noise attack density is increased, the PSNR values of NN wit r=1 also get affected, that is, they provide lower PSNR values. However, at increased noise attacks the second proposed filter provides better results at high noise attacks.

Further, we have selected first nine mages of the dataset [18]. Logically, PSNR values should be lower at high noise attacks. But, here the case is different for some images. As seen in the Table 1, for IPK 3*3 the PSNR value of Te-n0_0018 at 9% of noise attack is 35.1821. However, for images such a Te-n0_0017 and Te-n0_0016 the PSNR values are 33.3038 and 30.9811 at 8% and 7% noise attacks respectively. This is because the dataset contains a variety of brain images and in that some images are simple and some images are complex, or some images have high intensity and some images have low intensity or some images are blackish and some images are grayish. That is the reason that they provide different PSNR values. Thus, we also determined the average (avg) PSNR values. As shown in the table1, the avg PSNR values of the proposed methods are also better than the standard MF and SMF. Similarly, we conducted one experiment on same test image on varied SPN density. Table 2 presents the avg PSNR results and this analysis again showed that the proposed CA based denoising methods perform better.

At high noise attacks, the extended neighborhoods work better as they contain large number of cells for determining a noise free cell. This is the reason that neighborhoods with r=2 works better as compared to the neighborhoods with r=1. Point to be noted that adding more space around the central cell doesn't mean that we get the better results. As can ben from the Table 1 that in IPK 5*5 we add more cells than the CANN, r=2 but it still performs week. So, arrangement of cells around the cell under investigation is important. Thus, median filter with cellular automata performs better.

Furthermore, the proposed methods are also computationally better as compared to the standard MF and SMF. For example, in MF with IPK 3*3, the number of pixels processed at each step are 9 whereas as in CA_MF with NN r=1, number of pixels processed at each step are just 5. Similarly, for SMF with IPK 5*5, the number of pixels processed at each step are 25 whereas in CA_SMF with NN r=2, number of pixels processed at each step are just 13. Thus, proposed filters require half of the computing space and time taken by the standard MF and SMF.

Figure 3 shows the visual results of the various filters on SPN 30%. It is shown that the proposed method produces the best results. Results are shown from top to bottom. Figures, (a1) represents the original image, (a2) represents the image degraded by 30% of SPN, (a3) represents denoising by standard MF, (a4) represents denoising by proposed CA based MF, (a5) represents denoising by SMF, and finally (a6) represents denoising using proposed CA_SMF. It is shown that the proposed CA_MF and CA_SMF represents the better results as compared to the standard MF and SMF.

5. Conclusions

In this paper we presented two effective CA-based noise filters known as CA_MF and CA_SMF. Although the proposed filters work similar to those of MF and SMF but provides better results. Proposed filters work in two stage and use two transition functions. First transition function is used when noise attack is less whereas second transition function is used when noise attack is high. Moreover, the proposed filters proved computationally efficient as compare to the standard filters by adopting NN of CA. By doing this, the number of pixels processed at each step are reduced to half. The proposed filters could be improved further by exploring other models of CA like Elementary CA, Totalistic CA, Linear CA, and so on.

Declarations:

Ethical Approval: not applicable.

Funding: None.

Availability of data and materials: Sequence data that supports the findings of this study have been collected from the sources mentioned in references 18 and 23.

Image name	% of noise attack	MF		CA_MF		SMF		CA_SMF	
		IPK (3*3)	IPK (5*5)	NN (r=1)	NN (r=2)	IPK (3*3)	IPK (5*5)	CANN (r=1)	CANN (r=2)
Te-no_0010	1%	36.4116	31.8591	**39.7377**	**34.4538**	40.9729	38.1625	**43.2857**	**39.7419**
Te-no_0011	2%	35.9988	32.2607	**38.5922**	**34.2271**	40.4905	39.5692	**41.5482**	**39.9103**
Te-no_0012	3%	35.9628	31.6395	**37.2711**	**33.6082**	40.1586	39.5088	**40.7500**	**39.6315**
Te-no_0013	4%	33.0838	28.3258	**34.5879**	**31.1276**	37.7310	36.2736	**38.1528**	**37.1607**
Te-no_0014	5%	33.1410	29.1653	**35.6406**	**32.2929**	35.8782	35.2737	**38.7044**	**36.4811**
Te-no_0015	6%	34.1453	28.7571	**34.1538**	**32.1886**	38.8809	36.8664	36.0446	**38.1550**
Te-no_0016	7%	30.9811	25.8720	**31.2112**	**29.0884**	35.2337	33.4176	33.6284	**38.1699**
Te-no_0017	8%	33.3038	29.9313	32.6321	**32.7198**	37.4385	37.1832	34.3943	**38.3129**
Te-no_0018	9%	35.1821	31.2954	31.3985	**34.0939**	38.4431	38.9638	31.3748	**39.8510**
	Avg=	**34.2455**	**29.9006**	**35.0250**	**32.6444**	**38.3586**	**37.2465**	**37.5425**	**38.6015**

Table 1: PSNR analysis on various test images

Image name	% of noise attack	MF		CA_MF		SMF		CA_SMF	
		IPK (3*3)	IPK (5*5)	NN (r=1)	NN (r=2)	IPK (3*3)	IPK (5*5)	CANN (r=1)	CANN (r=2)
Te-gl_0010	1%	35.4816	30.2906	**39.2447**	**39.0667**	40.8909	**38.2297**	43.0833	**39.6338**
Te-gl_0010	2%	35.2608	30.2767	**38.6621**	**38.7085**	40.5544	**38.1492**	43.0135	**39.2366**
Te-gl_0010	3%	35.1494	30.1949	**37.9855**	**37.9388**	39.4765	**38.0926**	40.7958	**39.3458**
Te-gl_0010	4%	34.9371	30.1810	**37.1821**	**36.6473**	38.2230	**38.1551**	38.7907	**39.2012**
Te-gl_0010	5%	34.7637	30.1549	**36.4401**	**35.6404**	38.9176	**37.9537**	37.0686	**39.1981**
Te-gl_0010	6%	34.2236	30.0487	**34.7556**	**34.4084**	38.1426	37.5381	35.1971	**38.4886**
Te-gl_0010	7%	34.1921	30.1065	33.5561	**33.8715**	36.9994	37.2744	34.5539	**37.9977**
Te-gl_0010	8%	33.9465	30.0495	31.6413	**31.6403**	36.5621	37.2819	32.6305	**37.4066**
Te-gl_0010	9%	33.9264	29.9388	30.4654	**30.7131**	35.8870	36.1973	31.9812	**37.2445**
Te-gl_0010	**Avg=**	34.653	30.1379	**35.5481**	**35.4038**	38.4059	37.6524	37.4571	**38.6392**

Table 2: PSNR analysis on single test image

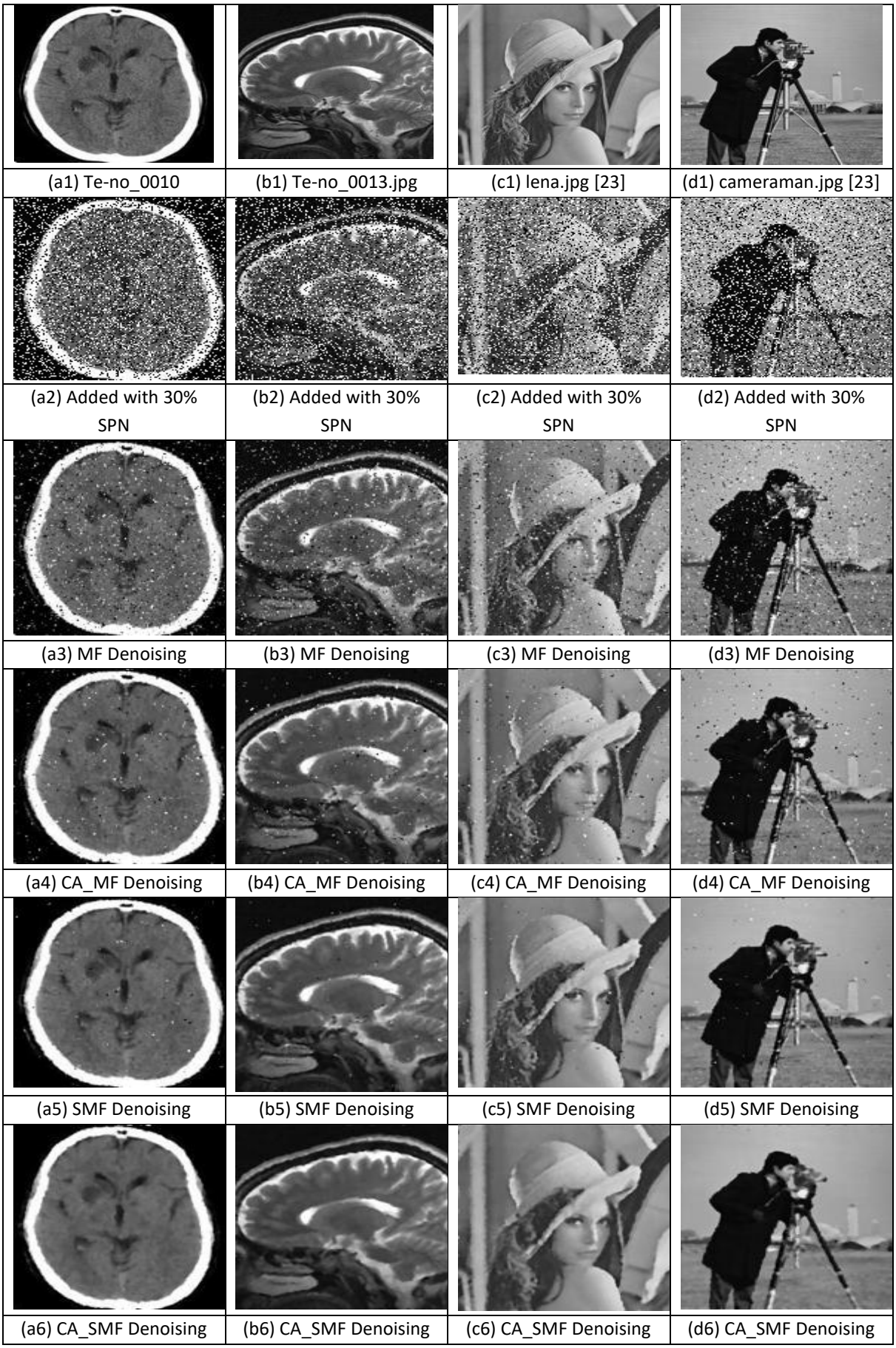

(a1) Te-no_0010	(b1) Te-no_0013.jpg	(c1) lena.jpg [23]	(d1) cameraman.jpg [23]
(a2) Added with 30% SPN	(b2) Added with 30% SPN	(c2) Added with 30% SPN	(d2) Added with 30% SPN
(a3) MF Denoising	(b3) MF Denoising	(c3) MF Denoising	(d3) MF Denoising
(a4) CA_MF Denoising	(b4) CA_MF Denoising	(c4) CA_MF Denoising	(d4) CA_MF Denoising
(a5) SMF Denoising	(b5) SMF Denoising	(c5) SMF Denoising	(d5) SMF Denoising
(a6) CA_SMF Denoising	(b6) CA_SMF Denoising	(c6) CA_SMF Denoising	(d6) CA_SMF Denoising

Figure 3: Denoising results of various test images used in this study.

References:

[1] A. C. Bovik, Handbook of Image and Video Processing. NY, USA: Academic, 2000.

[2] Gonzalez RC, Woods RE (2007) Digital image processing, 3rd edn. Prentice Hall, Englewood Cliffs

[3] B. Goyal, A. Dogra, S. Agrawal, and B. S. Sohi, "Noise Issues Prevailing in Various Types of Medical Images," Biomedical and Pharmacology Journal, vol. 11, no. 3, pp. 1227–1237, Sep. 2018, doi: 10.13005/bpj/1484.

[4] A. Shah et al., "Comparative analysis of median filter and its variants for removal of impulse noise from gray scale images," Journal of King Saud University - Computer and Information Sciences, vol. 34, no. 3, pp. 505–519, Mar. 2022, doi: 10.1016/j.jksuci.2020.03.007.

[5] K. Toh, H. Ibrahim, and M. Mahyuddin, "Salt-and-pepper noise detection and reduction using fuzzy switching median filter," IEEE Transactions on Consumer Electronics, vol. 54, no. 4, pp. 1956–1961, Nov. 2008, doi: 10.1109/tce.2008.4711258.

[6] Fei Duan and Yu-Jin Zhang, "A Highly Effective Impulse Noise Detection Algorithm for Switching Median Filters," IEEE Signal Processing Letters, vol. 17, no. 7, pp. 647–650, Jul. 2010, doi: 10.1109/lsp.2010.2049515.

[7] P. Zhang and F. Li, "A New Adaptive Weighted Mean Filter for Removing Salt-and-Pepper Noise," IEEE Signal Processing Letters, vol. 21, no. 10, pp. 1280–1283, Oct. 2014, doi: 10.1109/lsp.2014.2333012.

[8] Y. Wang, R. Adhmai, J. Fu, and H. Al-Ghaib, "A novel supervised learning algorithm for salt-and-pepper noise detection," International Journal of Machine Learning and Cybernetics, vol. 6, no. 4, pp. 687–697, Jun. 2015, doi: 10.1007/s13042-015-0387-9.

[9] H. Ma and Y. Nie, "A two-stage filter for removing salt-and-pepper noise using noise detector based on characteristic difference parameter and adaptive directional mean filter," PLOS ONE, vol. 13, no. 10, p. e0205736, Oct. 2018, doi: 10.1371/journal.pone.0205736.

[10] Y. Dai et al., "Improving adversarial robustness of medical imaging systems via adding global attention noise," Computers in Biology and Medicine, vol. 164, p. 107251, Sep. 2023, doi: 10.1016/j.compbiomed.2023.107251.

[11] S. V. Mohd Sagheer and S. N. George, "A review on medical image denoising algorithms," Biomedical Signal Processing and Control, vol. 61, p. 102036, Aug. 2020, doi: 10.1016/j.bspc.2020.102036.

[12] J. Ebrahimnejad and A. Naghsh, "Adaptive Removal of high-density salt-and-pepper noise (ARSPN) for robust ROI detection used in watermarking of MRI images of the brain," Computers in Biology and Medicine, vol. 137, p. 104831, Oct. 2021, doi: 10.1016/j.compbiomed.2021.104831.

[13] Z. Jeelani and F. Qadir, "Cellular automata-based approach for salt-and-pepper noise filtration," Journal of King Saud University - Computer and Information Sciences, vol. 34, no. 2, pp. 365–374, Feb. 2022, doi: 10.1016/j.jksuci.2018.12.006.

[14] S. Wolfram, "Statistical mechanics of cellular automata," Reviews of Modern Physics, vol. 55, no. 3, pp. 601–644, Jul. 1983, doi: 10.1103/revmodphys.55.601.

[15] M. A. Peer, F. Qadir, and K. A. Khan, "Investigations of Cellular Automata Game of Life Rules for Noise Filtering and Edge Detection," International Journal of Information Engineering and Electronic Business, vol. 4, no. 2, pp. 22–28, Apr. 2012, doi: 10.5815/ijieeb.2012.02.04.

[16] P. L. Rosin, "Image processing using 3-state cellular automata," Computer Vision and Image Understanding, vol. 114, no. 7, pp. 790–802, Jul. 2010, doi: 10.1016/j.cviu.2010.02.005.

[17] K. Bhattacharjee, N. Naskar, S. Roy, and S. Das, "A survey of cellular automata: types, dynamics, non-uniformity and applications," Natural Computing, vol. 19, no. 2, pp. 433–461, Jul. 2018, doi: 10.1007/s11047-018-9696-8.

[18] Msoud Nickparvar. (2021). Brain Tumor MRI Dataset, Kaggle. https://doi.org/10.34740/KAGGLE/DSV/2645886.